NH_3-SCR over V−W/TiO_2 Investigated by Operando X-ray Absorption and Emission Spectroscopy

Doronkin, D. E.; Benzi, F.; Zheng, L.; Sharapa, D. I.; Amidani, L.; Studt, F.; Roesky, P. W.; Casapu, M.; Deutschmann, O.; Grunwaldt, J.-D.;

Originally published:

May 2019

Journal of Physical Chemistry C 123(2019), 14338-14349

DOI: https://doi.org/10.1021/acs.jpcc.9b00804

THE JOURNAL OF PHYSICAL CHEMISTRY C

Subscriber access provided by UNIV OF SOUTHERN INDIANA

C: Surfaces, Interfaces, Porous Materials, and Catalysis

NH-SCR over V-W/TiO Investigated by *Operando* X-ray Absorption and Emission Spectroscopy

Dmitry E. Doronkin, Federico Benzi, Lei Zheng, Dmitry Sharapa, Lucia Amidani, Felix Studt, Peter W Roesky, Maria Casapu, Olaf Deutschmann, and Jan-Dierk Grunwaldt

J. Phys. Chem. C, **Just Accepted Manuscript** • DOI: 10.1021/acs.jpcc.9b00804 • Publication Date (Web): 24 May 2019

NH_3-SCR over V-W/TiO_2 Investigated by *Operando* X-ray Absorption and Emission Spectroscopy

Dmitry E. Doronkin[1,2], Federico Benzi[1], Lei Zheng[1], Dmitry I. Sharapa[2], Lucia Amidani[3,4], Felix Studt[1,2], Peter W. Roesky[5], Maria Casapu[1], Olaf Deutschmann[1,2], Jan-Dierk Grunwaldt[1,2,*]

[1]Institute for Chemical Technology and Polymer Chemistry (ITCP), Karlsruhe Institute of Technology (KIT), Engesserstraße 18, 76131 Karlsruhe, Germany

[2]Institute for Catalysis Research and Technology (IKFT), Karlsruhe Institute of Technology, Hermann-von-Helmholtz Platz 1, 76344 Eggenstein-Leopoldshafen, Germany

[3]The European Synchrotron Radiation Facility, BP 220, 38043 Grenoble Cedex, France

[4]present address: Helmholtz-Zentrum Dresden-Rossendorf, Institute of Resource Ecology, P.O. Box 510119, 01314 Dresden, Germany

[5]Institute of Inorganic Chemistry (AOC), Karlsruhe Institute of Technology (KIT), Engesserstraße 15, 76131 Karlsruhe, Germany

*Corresponding author: grunwaldt@kit.edu (J.-D. Grunwaldt).

Abstract

V-W/TiO_2 based catalysts, which are used for the removal of NO_x from the exhaust of diesel engines and stationary sources via Selective Catalytic Reduction with NH_3 (NH_3-SCR), were studied by *operando* X-ray absorption spectroscopy and emerging photon-in/photon-out techniques. In order to minimize the influence of highly X-ray absorbing tungsten and the fluorescence of titanium we used a high energy resolution fluorescence setup that is able to separate efficiently the V $K\beta_{1,3}$ emission lines and additionally allows to record valence-to-core (vtc) X-ray emission lines. The High Energy Resolution Fluorescence Detected X-ray Absorption Spectroscopy (HERFD-XAS) and vtc X-ray Emission Spectroscopy (vtc-XES) proved to be the only way to perform *operando* V K edge X-ray spectroscopic study on industrially relevant V-W/TiO_2 catalysts so far. The V-W/TiO_2 and V/TiO_2 samples were synthesized by incipient wetness impregnation and grafting and exhibit high activity towards NH_3-SCR. Raman spectroscopy showed that they mainly contained highly dispersed, isolated and polymeric V-oxo species. HERFD-XAS and XES identified redox cycling of vanadium species between V^{4+} and V^{5+}. With respect to most of the potential NH_3 adsorption complexes, DFT calculations further showed that vtc-XES is more limited than surface sensitive techniques such as infrared spectroscopy, Hence, a combination of X-ray techniques with IR or similar spectroscopies is required to unequivocally identify mechanism of NH_3-SCR over vanadia-based catalysts.

1. Introduction

Since the introduction of the Euro IV regulations, the engine optimization alone is no longer sufficient to reduce NO_x and particle matter emissions. The implementation of a well functioning catalytic exhaust aftertreatment system is thus required.[1] In modern heavy-duty diesel vehicles the selective catalytic reduction of NO_x by NH_3 (NH_3-SCR) is used as the state of the art method to decrease NO_x emissions. While certain systems, especially for the low temperature applications, are based on Cu- or Fe-zeolites,[2,3] a large number of heavy-duty diesel engines are equipped with vanadia-based SCR catalysts.[4–6] They are relatively inexpensive, stable against sulfur poisoning and can additionally oxidize hydrocarbons found in the diesel exhaust.[7]

V-W/TiO_2 catalysts are based on the anatase TiO_2 support material possessing high specific surface area, high acidity and high resistance to SO_2 poisoning.[8] To avoid the temperature induced anatase-rutile phase transformation, tungsten oxide (WO_3) is added as a structural promoter. In addition, tungsten oxide is known to show a positive effect on the activity of the catalyst by enabling higher dispersion of V and faster reoxidation of V species, higher number of acidic sites as well as improved resistance towards sulfur poisoning.[9–11] Vanadium oxide acts as the catalytically active species. Loadings between 0.5 and 1 monolayer of V species have been reported to lead to the highest catalytic activity[12,13] whereas V-oxo agglomerates or "islands" are less desirable.[10]

Understanding the reaction mechanism is essential, both for knowledge-based catalyst design and for process optimization. Unravelling the interaction between the reacting species (NO_x / NH_3) and the active V sites is an important step towards this goal. Hence, various *in situ* and *operando* techniques as well as density functional theory (DFT) calculations have been applied for more than two decades in order to identify the mechanism of NH_3-SCR over V catalysts. In pioneering *in situ* Fourier Transform Infrared Spectroscopy (FTIR) studies,

Topsøe[14] proposed a two-fold function of the V species. They act (a) as Brønsted acid sites (V-OH) for adsorption of NH_3 and (b) redox activation of adsorbed NH_x by a V=O group via hydrogen abstraction. However, no evidence for reaction of NO from the adsorbed state was found. Hence, an Eley-Rideal mechanism was proposed for NH_3-SCR and later validated using DFT calculations.[14–16] A DFT study by Yin et al. also supported the Topsøe dual-site mechanism.[17] Further FTIR studies by Ramis and Busca confirmed the general scheme with the exception that adsorption of NH_3 on Lewis rather than Brønsted acid sites was crucial for SCR,[18] and Marberger et al.[19] assigned active Lewis sites to mono-oxo vanadyl groups. With the help of DFT Vittadini et al.[20] noted that NH_3 can be adsorbed not only on V sites but also on Ti sites as a Lewis-acid-base adduct. Both types of adsorbed NH_x can contribute to the SCR pathway.[20] Tronconi et al.[21] investigated the kinetics of the SCR concluding that the vital function of V species is the redox function rather than provision of adsorption sites, suggesting the reaction cycle via reduction of V sites in the reaction between NO and NH_3 and their reoxidation by O_2 or NO_x. Using *in situ* EPR and Raman spectroscopy Due-Hansen et al.[22] could prove existence of significant amount of V^{4+} during SCR as well as its interconversion with V^{5+}, which demonstrates the redox transformations of vanadium. Further *operando* EPR and DRIFTS studies by Vuong et al.[23] support the Eley-Rideal mechanism, in which V species provide V^{5+}/V^{4+} redox pairs. Arnarson et al.[24] employed DFT calculations to formulate a consistent mechanism, in which NH_3 is adsorbed on a Brønsted site at the interface of Ti and V, while V^{5+} site provides redox functionality, i.e. accepts an electron during interaction of NO and adsorbed NH_4^+. Later the resulting V^{4+} site is reoxidized. Hence, there exists a general agreement on the redox role of V, although the experimental evidence is scarce and only obtained indirectly from *in situ* Raman and EPR studies. On the other hand, there is no agreement on the nature of sites for adsorption of NH_3, which can be V,[14–17] Ti,[20,24] or even sites formed by other dopants.[24] These uncertainties are a result of DRIFTS limited capability to distinguish between V and Ti adsorption sites, especially during catalyst working

in high water vapor environments requiring use of chemometric tools to separate H_2O and NH_3 bands.[25] Summing up, *operando* techniques allowing straightforward observation and quantification of redox dynamic of V sites as well as selective characterization of adsorbed species under realistic conditions (e.g. in the presence of water vapor) still need to be established for V-W/TiO_2 catalysts.

X-ray absorption spectroscopy (XAS) is a technique of choice for understanding changes in the oxidation state and coordination environment of active sites during real catalyst operation, i.e. *operando*. XAS and X-ray Emission Spectroscopy (XES) have already proven to be the proper techniques to probe the nature of Fe and Cu active sites in zeolite-based NH_3-SCR catalysts.[26,27] V K edge X-ray Absorption Near Edge Structure (XANES) region is very sensitive to the oxidation state and coordination environment,[28] which makes it also attractive for catalysis research. X-ray spectroscopy is element specific and has little interference from the environment such as the presence of water vapor, which is masking IR bands and hampering DRIFTS studies. A few *in situ* X-ray studies of V on SiO_2, TiO_2 and Al_2O_3 catalysts demonstrate redox dynamics of V sites,[29,30] while *ex situ* XANES was successfully used for the determination of the local environment of V.[4,31,32] Up to now, no *in situ* or *operando* XAS studies were performed on the realistic V-W/TiO_2 system. The reason lies in the complexity of the catalytic system nearly prohibiting conventional XAS. It is impossible to perform XAS measurements in the transmission mode due to the low energy of X-ray radiation at V K edge (5465 eV), which is absorbed by the W component in the catalyst. Conventional fluorescence measurements are also difficult to achieve due to the overlapping of V $K\alpha_{1,2}$ with the $K\beta_{1,3}$ lines of Ti, which prevails in the catalyst. The most suitable window material for the *in situ* cells, 0.01 mm thick quartz, absorbs approx. 35% of X-ray photons near V K edge energy further limiting the amount of photons reaching the detector. Hence, high photon flux sources are required. Fortunately, recent developments in photon-in /

photon-out hard X-ray techniques now allow *in situ* and *operando* X-ray spectroscopic measurements on V-W/TiO_2, by combining a source providing high photon flux and high resolution Johann-type X-ray fluorescence spectrometer, which allows resolving V $K\alpha_{1,2}$ and Ti $K\beta_{1,3}$ and probing only the V bands.[33] High Energy Resolution Fluorescence Detected (HERFD)-XANES allows more precise determination of oxidation states and coordination geometry of active sites, whereas valence-to-core X-ray Emission Spectroscopy (vtc-XES) may provide direct evidence for distinguishing the chemical nature of ligands (e.g. O or N) bound to the active site in question.[34–36] In this paper we present the first *operando* HERFD-XANES and vtc-XES study on a series of different conventionally impregnated and grafted V-W/TiO_2-catalysts[37] to identify dynamics of V oxidation state. In addition, we discuss possible adsorption of reagents / products of NH_3-SCR on V species using also prediction of spectral features based on DFT-optimized clusters.

2. Experimental

2.1 Sample Preparation

Two synthetic methods have been employed for the preparation of the catalysts, namely, incipient wetness impregnation and grafting. For the incipient wetness impregnation the support TiO_2 (Alfa Aesar, anatase) was calcined prior to the synthesis at 450 °C for 4 h in static air.[7] Afterwards the carrier was impregnated with ammonium metatungstate solution (pH value of 4-5), dried for 1 h at 80 °C, and calcined at 450 °C for 4 h. In a second step the ammonium metavanadate (Fluka) was dissolved in deionized water with addition of oxalic acid at 70 °C to obtain dark blue solution. The obtained solution was then used to impregnate the W/TiO_2 precursor obtained in the previous step. After impregnation the catalyst was dried at 80 °C for 1 h and calcined at 550 °C for 4 h. The impregnated sample is designated VWT.

Grafted samples were synthesized according to Reiche et al.[37] TiO_2 (anatase, Alfa Aesar, or anatase+rutile P25, Degussa/Evonik) was pre-conditioned at 10^{-4} bar and 150 °C for 3 h in a

quartz-glass flask. Tungsten was loaded via addition of tungsten (V) ethoxide (Alfa Aesar) in water-free hexane under stirring. The solution was stirred for 12 h at 50 °C. Afterwards, the solution was filtered and the remaining powder was washed five times with water-free hexane. Next, V was added in form of vanadyl trisisopropoxide (Alfa Aesar) in water-free hexane. Again, the solution was stirred for 12 h at 50 °C, filtered and the remaining powder washed five times with water-free hexane. The obtained powder was first calcined at 550 °C (400 °C for the sample without tungsten) for 4 h under N_2 atmosphere. In a last step, the obtained powder was calcined at 550 °C (400 °C for the sample without tungsten) for 2 h in air. The grafted samples are designated VWT-gr and VT-gr for the sample without W. Note that the grafted samples were synthesized by different groups using titania supports available in the corresponding groups.

2.2 Basic Characterization

The specific surface area of the powders was measured using N_2 physisorption at -196 ^oC on a Belsorp Mini II instrument (Bel Japan Inc.). All samples were degassed in vacuum at 300 ^oC before measurement. The specific surface area was estimated using the Brunauer, Emmett and Teller (BET) method.[38] The elemental composition was measured using inductively coupled plasma with optical emission spectroscopy (ICP-OES, OPTIMA 4300 DV, Perkin Elmer).

X-ray diffraction (XRD) patterns of the samples were collected in a 2θ range between 20^o and 80^o (step size 0.015°, 1 s per step) on a PANalytical X'pert PRO diffractometer with Cu K_α radiation. Raman spectroscopy was performed using a Renishaw inVia confocal Raman microscope. A Nd-YAG laser with a wavelength of 532 nm (100 mW) and a 2400 l/mm grating were used. Spectra were taken with 0.1% laser power and measurement times of 30 s. Approx. 80 spectra of several particles were measured which were averaged after cosmic ray removal using Renishaw WiRE software.

2.3. Catalysis

Catalytic performance was determined in a steady-state regime in a quartz tube plug flow reactor (ID 8 mm) and both the setup and some catalytic results have been reported in ref.[39] In brief, 250 mg sieved catalyst (150-300 μm) were mixed 250 mg SiO_2 (150-300 μm) for dilution to gain a total bed length of 10 mm. The gas hourly space velocity (GHSV, calculated with regards to the catalyst bed with SiO_2) was kept at 50 000 h^{-1}. Gases were dosed by individual mass flow controllers and volume concentrations were 500 ppm NO, 500 ppm NH_3, 5% H_2O, 10% O_2 in N_2 (Standard SCR) and 250 ppm NO, 250 ppm NO_2, 500 ppm NH_3, 5% H_2O, 10% O_2 in N_2 (Fast SCR). Prior to experiments the catalysts were heated to 550 °C in air (10 K/min ramp) after which air was replaced by the SCR feed and catalytic activity in Standard and Fast SCR was measured after stabilization of NOx and NH_3 concentrations (min. 30 min stabilization time). Then the reactor temperature was decreased stepwise and measurements were repeated. The gas composition was analyzed using a MultiGas 2030 FTIR gas analyzer (MKS Instruments). NO_x and NH_3 conversions were calculated using concentrations measured at the inlet and outlet of the catalytic reactor as follows:

$$X_{NOx} = 1 - \frac{(C_{NO}^{outlet} + C_{NO2}^{outlet} + C_{N2O}^{outlet})}{C_{NO}^{inlet} + C_{NO2}^{inlet}}, \quad (1)$$

$$X_{NH3} = 1 - \frac{C_{NH3}^{outlet}}{C_{NH3}^{inlet}}. \quad (2)$$

2.4. *Operando* HERFD-XANES / vtc-XES

HERFD-XANES and XES measurements were carried out at the ID26 beamline of the European Synchrotron Radiation Facility (ESRF, Grenoble, France). X-ray radiation was generated by three mechanically independent undulators and monochromatized by a cryogenically cooled Si (111) double-crystal monochromator. The emission spectrometer was

equipped with four spherically bent (r = 1 m) Ge (422) analyser crystals installed in a Rowland geometry and an avalanche photo-diode (APD) detector. The counts of the detector were normalized by a photodiode in front of the sample (I_0). The resulting instrumental energy bandwidth was below 1.5 eV, which is comparable to the natural width of the V K edge core hole (1.01 eV). The beam size was kept at 0.1 mm (vertical) x 0.6 mm (horizontal). Test scans with and without attenuators were recorded and the corresponding changes in conversion of the reactants with and without X-ray beam were evaluated to identify beam induced changes ("beam damage") in the samples (Figure S1). The beam-induced changes were deemed insignificant in this specific case (possibly due to high fraction of X-rays absorbed by the quartz capillary walls) and no beam attenuators were used to maximize counts.

The X-ray absorption spectra in terms of HERFD-XANES were measured by scanning the incident energy and detecting the fluorescence at the maximum of the V $K\beta_{1,3}$ emission line (5426.8 eV). Energy was calibrated by using a metallic vanadium foil. The X-ray emission spectra around the main ($K\beta_{1,3}$) and the satellite ($K\beta''/K\beta_{2,5}$) emission lines were recorded between 5408-5488 eV while applying excitation energy of 5613 eV.

The pre-edge features were extracted and analyzed from the XANES spectra by using an arctangent function to simulate the edge jump and relative broadening to extract the pre-edge from the normalized XANES spectrum (analogous to procedure reported by Farges et al.[40] and Giuli et al.[41]). A set of Pseudo-Voigt functions have been used to fit the pre-edge components. The centroid position and the intensity of each peak in the samples were recorded and compared to that of a set of V-bearing model compounds, representative of the most common V oxidation states and coordination geometries.

The satellite emission lines (vtc-XES) were extracted from the tail of $K\beta_{1,3}$ using Fityk software[42] analogous to a procedure reported by Gallo and Glatzel.[43] To extract the

background of the vtc region, the $K\beta_{1,3}$ line tail (excluding the vtc-XES lines which gives regions between 5428.5-5437 and 5470-5480 eV) was fitted using 4 Voigt functions centered between 5423 and 5426 eV. Then, the modelled tail function was subtracted from the valence-to-core experimental data. The vtc-XES spectra were normalized by the maximum intensity of the main ($K\beta_{1,3}$) lines.

For collecting *in situ* data a setup with a heated quartz capillary microreactor (plug flow geometry, diameter 1 mm, wall thickness 0.01 mm) was used.[44] The quartz capillary was heated with an air blower (Gas Blower GSB-1300, FMB Oxford) and tilted 45° with respect to the incident beam and analyzer crystals. The spectra were measured near the beginning of the catalyst bed unless stated otherwise. Pure gases and gas mixtures were dosed to obtain the desired volume concentrations: ca. 900-1000 ppm NO, 1000 ppm NO_2 (or 500 ppm NO + 500 ppm NO_2 for Fast SCR), 1000 ppm NH_3, 1000 C_3H_6, 5% O_2 and pure He as balance. The gas flow was kept at 50 mL/min which results in a GHSV of 660 000 h^{-1}. Water was dosed using a saturator and resulting in approx. 1.5% H_2O. Gas analysis was performed using an FTIR analyzer (MultiGas 2030, MKS Instruments). Before the measurements the catalysts were heated in He to 500 °C for 15 min and between exposures to different gas mixtures the catalysts were heated in 10% O_2/He to 500 °C for 15 min to reoxidize V sites and desorb any species potentially adsorbed during the previous experiment.

To obtain reference spectra pure chemicals (Aldrich) and mineral samples kindly provided by G. Giuli (Unicam) were pressed to self-supported wafers with BN. XANES spectra of the reference compounds have been previously reported by Benzi et al.[45] In order to minimize self-absorption effects in the XANES spectra VO_2 and V_2O_5 were mixed with BN to obtain 2 wt.% V in the resulting mixture (corresponding to V loading in the catalyst samples) and measured in Kapton® tubes (1.6 mm diameter). All spectra were nevertheless corrected for self-absorption by using the FLUO algorithm from the IFEFFIT package.[46]

2.5. Calculations of vtc-XES spectra

DFT structure optimization was performed with VASP 5.4.1[47] using BEEF-vdW[48] GGA functional. 3 3 1 K-points were taken and energy cutoff was set to 500eV. As a site for NH_3 adsorption single VO_x on TiO_2 support optimized by Arnarson et al.[49] was chosen. All atoms of the TiO_2 support except O atoms linked to V were fixed during the optimization. Starting adsorption geometries were identified based on the work by Yin et al.[50] and included Lewis adsorption on deeply reduced V site (without terminal O, L1 site) and oxidized vanadyl (L2 site) as well as Brønsted adsorption via terminal OH (B1) and one or two bridging O(H) which both degenerated to the structure B2 with NH_4^+ bound to a single bridging oxygen (see SI). The vtc-XES spectra of the resulting model structures were calculated using FEFF 9.6.4 software[51] and the corresponding input files are available in the SI.

3. Results and Discussion

3.1. Physico-Chemical Characterization of the Studied Catalysts

The composition and phases of the obtained catalysts are summarized in Table 1. The composition of the impregnated catalyst corresponds to that of catalysts typically used in industry, whereas the grafted samples were synthesized with the aim to produce less than a monolayer of V species on titania. Surface area (S_{BET}) of the impregnated VWT catalyst is 66 m^2/g and similar values were obtained for the grafted VWT-gr (57 m^2/g) and VT-gr (55 m^2/g) samples. Thus, a representative series including model and more realistic samples was obtained for the investigation of redox and structural dynamics of V-sites during SCR.

Table 1: Physico-Chemical Characterization of the Studied Catalysts

Catalyst	Synthesis technique	V loading, wt%	W loading, wt%	Surface area, m^2/g	Support phase	V species according to Raman
VWT	incipient wetness impregnation	3.5	11.1	66	anatase	polymeric vanadates, isolated vanadyls
VWT-gr	grafting	2.1	5.0	57	anatase	polymeric vanadates
VT-gr	grafting	2.1	-	55	anatase + rutile	polymeric vanadates

The XRD patterns shown in the Electronic Supplementary Information (ESI, Fig. S2a) exhibit reflections predominately from anatase TiO_2 phase in all catalysts. VT-gr also contains some rutile TiO_2 phase, typical for the used Degussa/Evonik P25 support.[52] No crystalline V_2O_5 or WO_3 phases were detected in the grafted VWT-gr and VT-gr catalysts. However, crystalline WO_3 was observed in the impregnated VWT catalyst.

Raman spectra in the full measured range are reported in the ESI (Fig. S2b). All samples display bands at 144, 197, 397, 515, 639, and 794 cm^{-1} attributed to the anatase phase of TiO_2.[53,54] The VT-gr sample also shows distinct features at 238, 362, and 445 cm^{-1} attributed

to the rutile TiO_2.[53] Furthermore, VT-gr shows a band at 319 cm^{-1}, while in the spectra of VWT and VWT-gr samples this band is located at 313 cm^{-1}, bands around 320 cm^{-1} were previously observed for both anatase and rutile TiO_2.[53] Fig. 1 shows the Raman spectra of the synthesized catalysts in the region of V-O vibrational bands. The VWT spectrum displays peaks at 886, 981, 1003, and 1020 cm^{-1}. The bands at 886 and 981 cm^{-1} may be assigned to asymmetric V-O-V bending and V=O stretching vibrations in polymeric vanadates, respectively.[55,56] The signal around 1003 cm^{-1} is rarely seen and was attributed to V=O stretching in polymeric V oxo species as well,[55,56] while the band at 1020 cm^{-1} originates from V=O stretching in isolated vanadyls.[10,37,56] The only peak at 981 cm^{-1} could be observed in the case of VWT-gr sample and was attributed to asymmetric V=O stretching vibrations in polymeric vanadates.[55,56] The VT-gr catalyst displays two peaks in the given area at 937 and 981 cm^{-1} both of which are attributed to polyvanadate chains bound to the TiO_2 support.

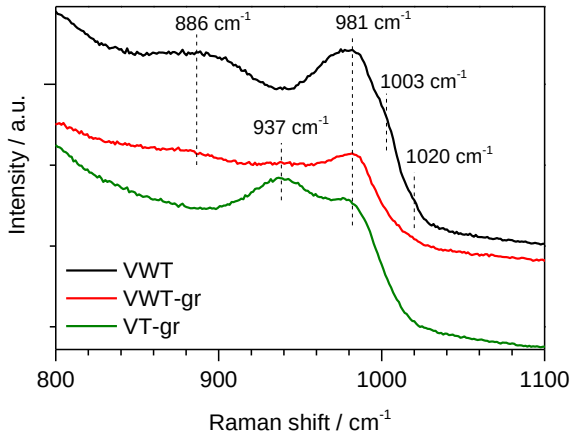

Figure 1. Raman spectra of the studied catalysts in the range of V-O vibrations.

3.2 Catalytic Performance in NH_3-SCR

The catalytic activity of the synthesized V(-W)-TiO_2 samples in Standard NH_3-SCR is illustrated in Fig. 2. All samples showed good activity, typical for V-W-TiO_2 catalysts.[4,7,57] The impregnated VWT sample had a higher performance at low temperature but also more active in unselective oxidation of NH_3. The latter resulted in lower NO_x conversion at high

temperature. This may be assigned to presence of less SCR-active and less selective 3-dimensional vanadium oxide aggregates in this catalyst.[4,10] Grafted catalysts demonstrated somewhat lower SCR activity below 300 °C but higher selectivity above 450 °C. No significant effect of W or the TiO_2 phase composition on the activity of the grafted catalysts was noticed. Its presence might be more relevant for the hydrothermal stability of the catalysts, which was not the goal of the current work. With the activity data we have set the basis for a representative series of catalysts containing high fraction of active V species suitable for the advanced V K-edge X-ray spectroscopic studies.

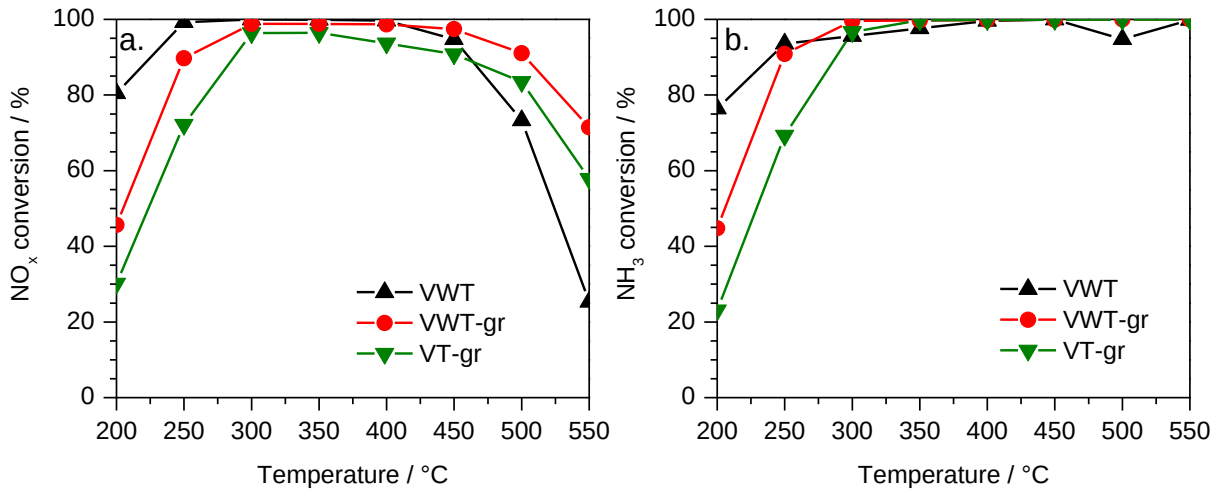

Figure 2. (a) NO_x and (b) NH_3 conversion profiles obtained using lab bench reactor during Standard SCR over tested catalysts. Conditions: 500 ppm NO, 500 ppm NH_3, 5% H_2O, 10% O_2 in N_2. GHSV 50 000 h^{-1}.

Operando investigations strongly require proving that the catalyst is actually working during measurements. For this purpose, the concentrations of gaseous species at the outlet of the capillary microreactor cell were monitored during the XAS / XES studies. The resulting conversions correspond to the typical behavior of V catalysts[10] in NH_3-SCR at high space velocity and are reported in Fig. 3. No significant effect of exposure to the X-ray beam (i.e. indication of "beam damage") on the conversion was found (Figure S1).

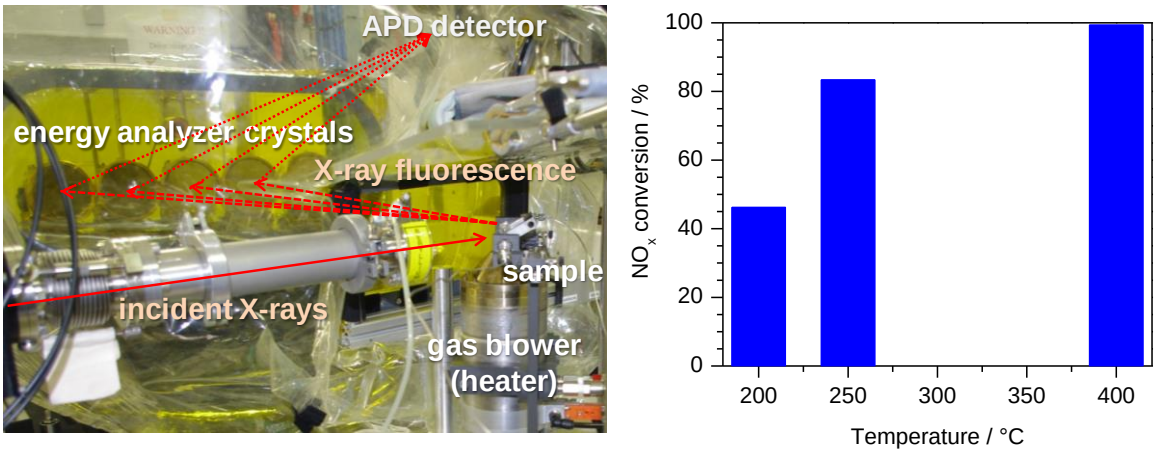

Figure 3. Spectroscopic setup for HERFD-XAS and XES (photo with decisive components) at beamline ID26 (ESRF, Grenoble) and NO_x conversions during Standard SCR of a VWT catalyst in the capillary microreactor. Conditions: 900 ppm NO, 1000 ppm NH_3, 1.5% H_2O, 5% O_2 in He. GHSV 660 000 h^{-1}.

3.3 *Operando* HERFD-XANES / XES of the Impregnated Catalyst under Various Test Conditions and NH_3-SCR

The impregnated VWT catalyst was chosen for the detailed mechanistic studies as a typical example of V-based NH_3-SCR catalysts. For XAS and XES techniques it is important to maximize the amount of active species because the X-ray absorption and emission spectra origin from all atoms of a certain element and, thus, contain averaged information from active and inactive species.[27] Hence, in order to highlight possible structure and oxidation state variations during SCR at low but also elevated temperatures[26] we mainly focused on measuring X-ray spectra at the beginning of the catalyst bed.

For data analysis and for quantification purposes, spectra of several reference compounds (V oxides and V-bearing minerals containing V^{3+}, V^{4+}, and V^{5+} with 4 to 6 fold coordination) were measured. The recorded basic set of X-ray absorption and emission spectra of V_2O_3, VO_2, and V_2O_5 is shown in Fig. 4 and they strongly change. Consistent shifts in the positions of the emission lines (Figs. 4a, 4b) can be attributed to changing V oxidation state. Of these,

core-to-core $K\beta_{1,3}$ emission lines (Fig. 4a) are only weakly sensitive to the ligand environment and can be used to derive oxidation states of transition metals.[58] Position of the rising edge in the XANES spectra (Fig. 4c) depends on the oxidation state of V. Position and intensity of the pre-edge peak at approx. 5470 eV can also be used to evaluate oxidation state and coordination number of V sites.[45] Altogether, several features in the V K edge XANES spectra can be used to evaluate oxidation state of V, however, they all should be treated with caution because of sensitivity of XANES to the coordination geometry.

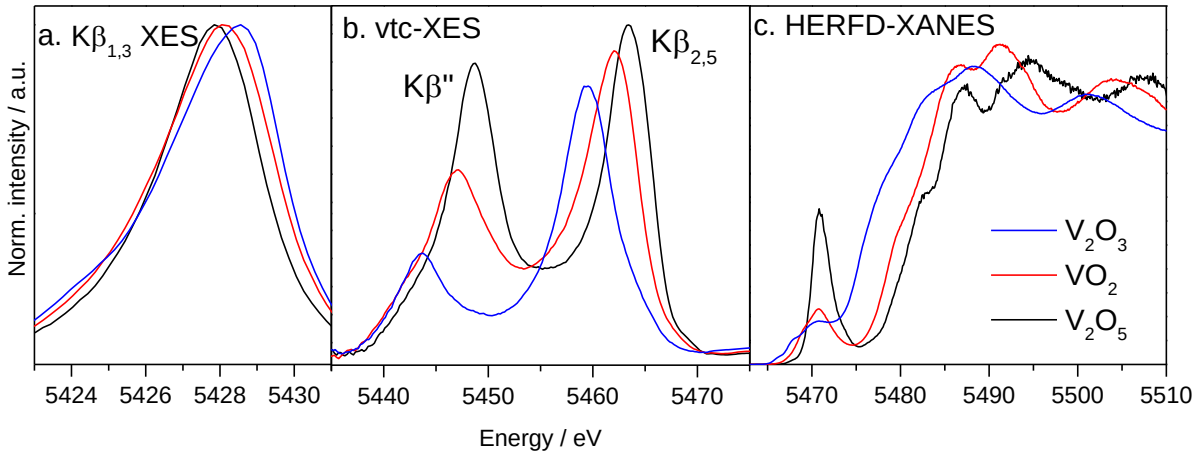

Figure 4. XES and HERFD-XANES spectra of V_2O_3, VO_2 and V_2O_5 reference compounds.

In order to evaluate behavior of V sites in V-W/TiO_2 catalysts under model and realistic SCR-related conditions, we defined a large number of test conditions including single reactant gases and their mixtures as well as mixtures containing exhaust gas components influencing activity and / or selectivity of V SCR catalysts, e.g. water and hydrocarbons. The exhaustive list of the test conditions alongside with the results of the evaluation of the obtained XES and XAS spectra is given in Table 2. O*perando* spectra of the VWT catalyst under these test conditions showed only minor variations. Hence, for clarity, only the selected spectra recorded under SCR as well as conditions inducing the biggest spectral changes are shown in Fig. 5. While changing from oxidizing feeds (O_2/He, NO+O_2/He) to the reducing feed (NH_3/He) only shifts in the position and decrease of the intensity of emission peaks as well as of the pre-edge and the rising edge were observed. Contrary to the case of the zeolite-based

catalysts,[34,35] no additional features appeared in vtc-XES or XANES spectra and only shifts in peak positions were observed, in line with shifts in the spectra of VO_2 and V_2O_5 reference compounds (Fig. 4a,b). This allows drawing a preliminary conclusion that switching between oxidizing and reducing feeds leads to variations in oxidation state of V sites but probably with only minor changes of the coordination sphere of V (e.g. due to potential adsorption of NH_3 on V). We observed this both for the reaction feeds and the NH_3 only feed (NH_3/He) in which high coverage of NH_3 adsorption sites is to be expected and was earlier reported by DRIFTS.[14–19]

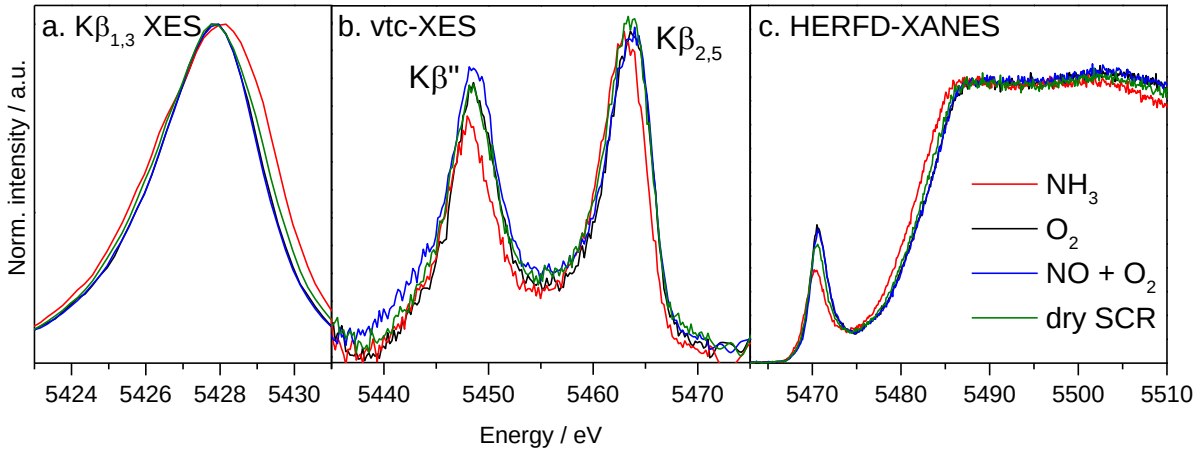

Figure 5. *Operando* (a) $K\beta_{1,3}$ XES, (b) vtc-XES and (c) HERFD-XANES spectra of the impregnated VWT catalyst during dry SCR (900 ppm NO, 1000 ppm NH_3, 5% O_2 in He, no water vapor) and in related model gas mixtures (diluted with He). Temperature 250 °C.

Analysis of the XANES pre-edge features can be furthered with the help of a so-called variogram. The variogram is a plot of the absolute intensity of pre-edge peaks versus their centroid position, which allows semi-quantitative estimation of oxidation state and coordination number of elements in question.[34,40,41,59] The lines ("mixing lines") connecting points with equal oxidation states or coordination numbers are calculated from the linear combination of the reference spectra (of model compounds) with the corresponding molar fractions of element in question, i.e. vanadium.[34,41,59] The oxidation state and coordination

geometry of an unknown sample are then estimated by comparing its pre-edge peak intensity and position against the library of model compounds and the corresponding mixing lines. The mixing lines form a grid allowing semi-quantitative speciation of intermediate species with respect to the model compounds. Noteworthy, the position and intensity of the pre-edge features are also influenced by the spin state[60] of the corresponding metal which may further limit the accurate quantification.

The exemplary variogram drawn from the spectra of the VWT sample under the most extreme SCR-related conditions at 250 °C is shown in Fig. 6a. The experimental points are located near a mixing line showing 5-fold coordinated vanadium sites with an oxidation state between 4 and 5. Hence, the pre-edge analysis shows oxidation or reduction of V sites under NO_x or NH_3 but very small to no changes in the coordination of V species (as the experimental datapoints do not significantly deviate from the mixing line). Only if the catalyst is exposed to NH_3/He the data point overlaps with a mixing line for a CN 5, while the others are shifted in the area of slightly lower coordination numbers. During the Standard SCR test some excess of NH_3 was dosed resulting in NH_3 slip. This might have influence on the value of V oxidation state but it did influence much less the coordination environment of V sites. Thus, the data set obtained from XANES at 250 °C indicates a redox response but does not reveal significant changes in the coordination sphere of V sites under SCR-related conditions.

Based on the variogram (Fig. 6), values of V oxidation state and coordination number were estimated from the HERFD-XANES spectra measured under model gas mixtures, Standard and Fast NH_3-SCR, with and without water vapor as well as with and without C_3H_6, and also during SCR with C_3H_6 as the only reductant (Table 2). Oxidation state of V was also obtained from fitting the $K\beta_{1,3}$ emission line by a linear combination of $K\beta_{1,3}$ lines from the XES spectra of cavansite (V^{4+}) and V_2O_5 references (both normalized by the height). All available

$K\beta_{1,3}$ reference spectra are summarized in Fig. S4a; the choice of reference compounds (cavansite and V_2O_5) was based on the best fit criterion (Fig. S4b,c).

Table 2. Average Oxidation States and Coordination Numbers of V in the VWT Catalyst under SCR and Related Conditions at 250 °C. Spectra were Measured at the Beginning of the Catalyst Bed.

Experiment	Gas mixture	V oxidation state (from pre-edge / from XES)	V coordination number
0	He only	4.4 / 4.7	<5
1	O_2	4.6 / 4.9	<5
2	NO	4.6 / 4.9	<5
3	$NO+O_2$	4.65 / 4.9	5
4	O_2+H_2O	4.5 / 4.9	<5
5	$NO+O_2+H_2O$	4.55 / 4.9	<5
6	NH_3 (water-free)	4.2 / 4.4	5
7	NH_3+O_2	4.45 / 4.7	<5
8	$NH_3+O_2+H_2O$	4.45 / 4.7	<5
9	$C_3H_6+H_2O$	4.2 / 4.5	<5
10	$C_3H_6+O_2+H_2O$	4.4 / 4.7	<5
11	$NH_3+C_3H_6+O_2+H_2O$	4.3 / 4.7	<5
12 (dry SCR)	$NO+O_2+NH_3$	4.45 / 4.7	<5
13 (SCR)	$NO+O_2+NH_3+H_2O$	4.35 / 4.8	<5
14 (HC-SCR)	$NO+O_2+C_3H_6+H_2O$	4.45 / 4.8	<5
15 (NH_3+HC-SCR)	$NH_3+NO+O_2+C_3H_6+H_2O$	4.35 / 4.7	<5
16 (Fast NH_3+HC-SCR)	$NH_3+NO+NO_2+O_2+C_3H_6+H_2O$	4.4 / 4.75	<5
17 (Fast SCR)	$NO+NO_2+O_2+NH_3+H_2O$	4.45 / 4.8	<5

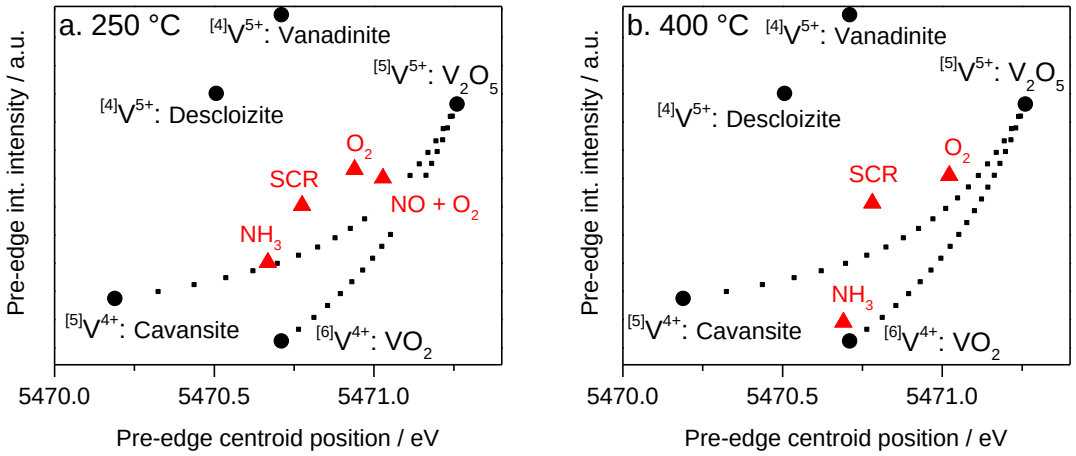

Figure 6. Plot of the pre-edge intensity (area) and the centroid position (area-based average position) extracted from HERFD-XANES spectra of reference compounds representative of V^{4+} and V^{5+} with 4-, 5- and 6-fold coordination (circles), their binary linear combinations (mixing lines) and the VWT catalyst under the most oxidizing / reducing SCR-related conditions at (a) 250 °C and (b) 400 °C (triangles). Coordination numbers of V in the reference compounds are reported in brackets as a superscript preceding the V sign, e.g. $^{[5]}$V.

The data in the Table 2 does not show any significant changes in the local coordination of V sites, which is in agreement with the recent DFT and EPR results.[49] Depending on the atmosphere, V^{5+} sites undergo reduction to V^{4+}, which is the strongest for interaction with NH_3 (exp. 6) or C_3H_6 (exp. 9). A small difference between the two experiments is that with C_3H_6 only V^{5+} reduction is observed, while interaction with water-free NH_3 leads also to a small increase in the coordination number (exp. 6). This increase is not observed if other SCR-reactants are added to the feed. Under SCR conditions V shows intermediate oxidation states with a typical gradient from the more reduced beginning to the more oxidized end of the catalyst bed as was revealed for zeolite SCR catalysts.[26,34,35]

V coordination number under almost all conditions remains unchanged at approx. 5 indicating square pyramidal V complexes.[49] Thus, V sites show dynamic oxidation state during SCR and, unlike the transition metals in zeolites, hardly any changes in the first coordination shell.

Note furthermore that heating the sample under NH_3 oxidation feed (exp. 8) or SCR feed (exp. 13) to 400 °C does not change the observed trend, with no significant shifts or new features also in the vtc-XES spectra. In contrast, exposure to NH_3/He feed at 400 °C leads to a deep reduction of V^{5+} to V^{4+} (Table 3) and a coordination number of 6 (Fig. 6b) but this is not the case for other feeds (most importantly, the SCR feed) which show the same spectra as at 250 °C. DFT modeling predicted 5-fold coordination of V (square pyramidal geometry with 5 O atoms at approx. 2 Å) and one additional O atom at a distance of approx. 2.8 Å.[49] Deep reduction of V by NH_3 may cause shortening of the 6th V-O bond effectively leading to nearly octahedral VO_6 units[63] which is also visible in the variogram as the increase in the coordination number. Hence, this increase may stem from reduction of V^{5+} to V^{4+} but weak Lewis adsorption of NH_3 is not excluded as will be shown in the following section.

Concerning the influence of other species found in the diesel exhaust, e.g. water or hydrocarbons, no significant changes were observed when these species were added to the SCR reaction feed. Only hydrocarbon (C_3H_6) addition during SCR (exp. 15) resulted in a higher reduction degree of V compared to the HC-free SCR (exp. 13, XES result). Addition of C_3H_6 is known to decrease SCR activity of VWT,[7] the explanation of this poisoning effect may be hydrocarbon-induced inhibition of reoxidation of V^{4+} sites necessary for completion of the SCR cycle.[21]

3.4 Nature of Nearest Neighbors around V Sites According to vtc-XES

Previous studies of Fe- and Cu-zeolite catalysts revealed profound differences in the vtc-XES and HERFD-XANES spectra recorded under model SCR-related gas media such as in NH_3/He and NO_x(+O_2)/He. [34,35,64,65] The differences were related to the shape and positions of Kβ" and $K\beta_{2,5}$ emission lines, appearance of additional Kβ" emission lines due to interaction of NH_3 with the studied metals and to appearance / disappearance of features in the pre-edge and rising edge regions of the XANES spectra. In all cases, the changes were associated with

the oxidation and reduction as well as adsorption-desorption of species at the active site. The spectra measured during SCR (also involving realistic gas mixtures, e.g. with water vapor), in turn, showed averaged features from both NH_3/He and $NO_x(+O_2)$/He model cases and are more difficult to interpret. Thus, the most significant variations in the current study are expected to be observed under model NH_3/He and in NO_x/He gas feeds.

The rather small shifts of Kβ" and $K\beta_{2,5}$ emission lines (Fig. 5b) in different gas mixtures cannot be attributed to a change in the nature of nearest neighbors since energy shifts in V Kβ" XES may amount to 5-10 eV.[29] This is compared to the Fe and Cu XES spectra in which the Kβ" energy shifts when replacing O with N neighbors amount to 3 and 1.4 eV correspondently.[34–36] In order to support this conclusion and also to examine whether the adsorption of NH_3 via an OH group (Brønsted site) may lead to the observed changes we also calculated vtc-XES spectra of a model V site with several different NH_3 adsorption geometries summarized in Fig. S3. Two Lewis adsorption modes were optimized by DFT in which NH_3 is adsorbed instead of the terminal O of the vanadyl group (L1, E_{ads} = -1.4 eV) and NH_3 approaching the vanadyl group from the side with H atoms aligned to oxygen atoms of the VO_x entity (L2, E_{ads} = -0.4 eV). In addition, Brønsted adsorption modes were simulated with NH_4^+ bound via terminal (B1, E_{ads} = -1.6 eV) or one bridging oxygen (B2, E_{ads} = -2.1 eV). A model with NH_4^+ forming two hydrogen bonds to two bridging oxygen atoms[50] is unstable and rearranges to the B2 model. The calculated spectra (Fig. 7) show only two emission peaks for nearly all adsorption configurations. Only in case of strong reduction of the vanadyl group and the subsequent direct Lewis adsorption and V-N bond formation (L1 model, Fig. 7a) a weak third emission peak appears in the vtc-XES spectrum. This peak attributed to a transition from the lone pair of N in NH_3 to the core-hole at V and was experimentally observed during propane ammoxidation by Safonova et al.[29] However, in our case SCR-related reducing conditions are probably too mild to abstract O from the vanadyl

group and form the L1 adsorption complex. As a result, we do not observe any significant amount of this complex in the vtc-XES spectra. L2 complex (NH_3 approaching the vanadyl group from the side) cannot be excluded based on the vtc-XES spectra and it may explain the increased coordination number observed in dry NH_3/He atmosphere.

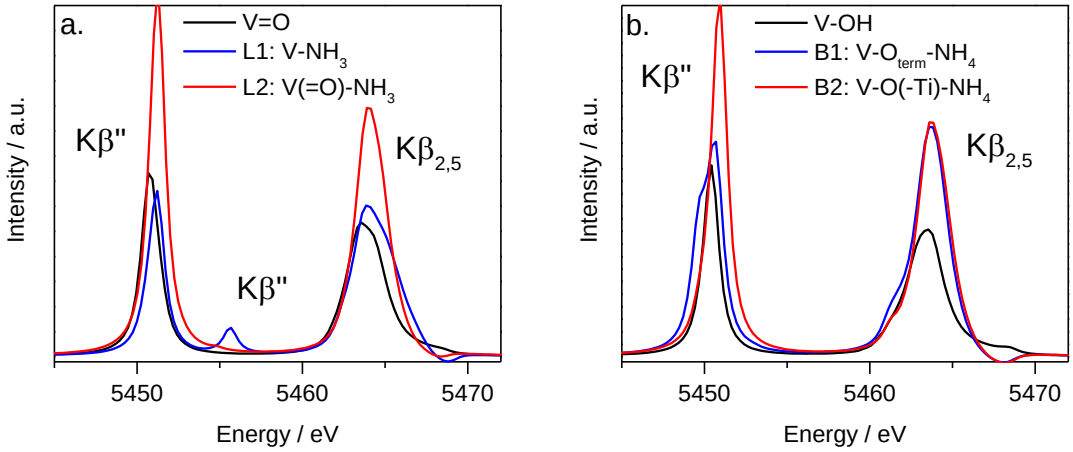

Figure 7. Calculated vtc-XES spectra based on DFT-optimized V site models with adsorbed NH_3: (a) comparing direct V-O and V-N interaction, i.e. Lewis adsorption modes, and (b) corresponding NH_3 adsorption on Brønsted V-OH site.

Ammonia may also be adsorbed as NH_4^+ via O (Brønsted adsorption). Brønsted adsorbed ammonia has been observed by DRIFTS[19,66] and predicted by DFT calculations.[17,24] It should be noted that while both TiO_2 and VO_x can provide Lewis adsorption sites no Brønsted sites occur on pristine TiO_2.[67,68] Hence Brønsted-bound ammonia observed in DRIFTS experiments may only be bound to VO_x species. We set up two models with Brønsted-bound ammonia and calculated the respective vtc-XES spectra summarized in Fig. 7b. The spectra suggest small shifts of Kβ" lines but no splitting of Kβ" so that Brønsted adsorbed ammonia would not be visible in the experimental vtc-XES spectra (Fig. 5b). Thus, we attribute the observed small shifts in the experimental spectra (Fig. 5b) to the redox dynamics of V species and Brønsted adsorption of NH_3 on VO_x sites. Based on vtc-XES data alone, even weak Lewis adsorption (L2 configuration) of ammonia cannot be excluded. However, the DRIFTS

study of Zhu et al.[66] proved that at medium to high V loadings such as used in this study Brønsted adsorption sites form the majority of all NH_3 adsorption sites.

3.5 *Operando* HERFD-XANES / vtc-XES on Grafted Catalysts

Since changes in the first coordination shell of V sites in the impregnated VWT catalyst during SCR at 250 °C were marginal, we further investigated grafted V catalysts that exhibit VO_x chains / monolayer V sites active in SCR. This approach aimed at maximizing the fraction of V sites exposed to the reactants of the SCR, and consequently to maximize SCR-induced spectral changes. Measurements of the VWT-gr catalyst at 250 °C demonstrated even weaker spectral response to changing gas feeds compared to the impregnated VWT. Hence, the comparison was extended to 400 °C only under the most oxidizing and the most reducing feed conditions. The obtained spectra are displayed in Figs. 8 (VWT-gr catalyst) and 9 (VT-gr catalyst) and oxidation states / coordination numbers are summarized in Table 3 (variograms are available in the ESI, Figs. S5 and S6).

Table 3. Average Oxidation States and Coordination Numbers of V in the Measured Series of Catalysts under Varying Gas Atmospheres at 400 °C. Spectra under SCR Conditions are Measured at the Beginning of the Catalyst Bed. Other Measurements were Done in the Middle of the Catalyst Bed.

Exp. no.	Gas mixture	Catalyst					
		VWT		VWT-gr		VT-gr	
		Ox. state. (pre-edge / XES)	Coord. no.	Ox. state. (pre-edge / XES)	Coord. no.	Ox. state. (pre-edge / XES)	Coord. no.
1	O_2	4.65 / 5.0	~4.5	4.7 / 4.9	<5	4.5 / 4.3	~5.7
2	$NO+O_2$	n.a.		4.7 / 4.9	≤5	4.5 / 4.4	~5.7
3	NH_3	4.0 / 4.0	6	4.4 / 4.5	<5	4.2 / 4.2	5.75
4	SCR*	4.4 / 4.8	<5	4.65 / 4.85	≤5	4.5 / 4.4	~5.7

*for VWT sample SCR with water vapor is reported, for other catalysts – dry SCR

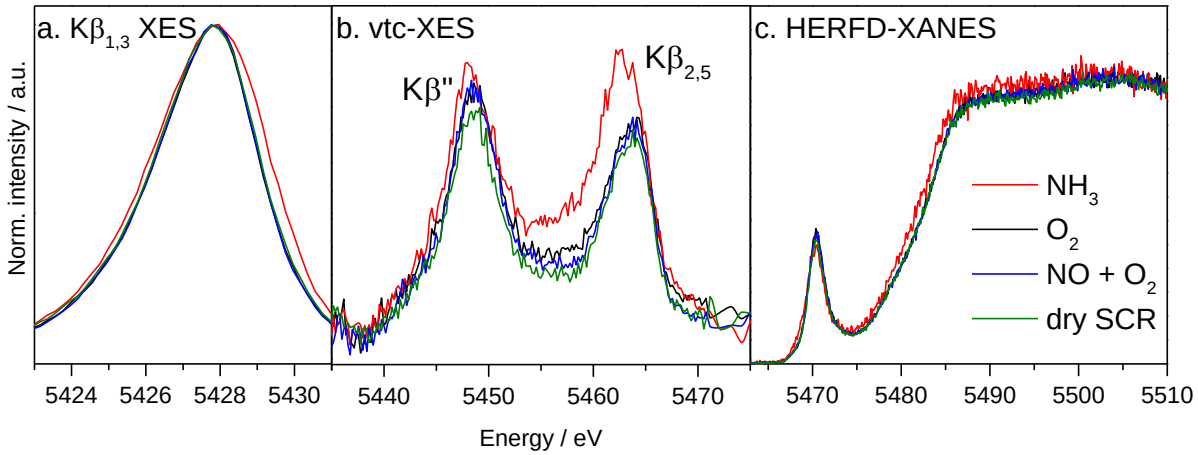

Figure 8. *Operando* (a) Kβ$_{1,3}$ XES, (b) vtc-XES and (c) HERFD-XANES spectra of the grafted VWT-gr catalyst during dry SCR (1000 ppm NO, 1000 ppm NH_3, 5% O_2 in He, no water vapor) and in related model gas mixtures (diluted with He). Temperature 400 °C.

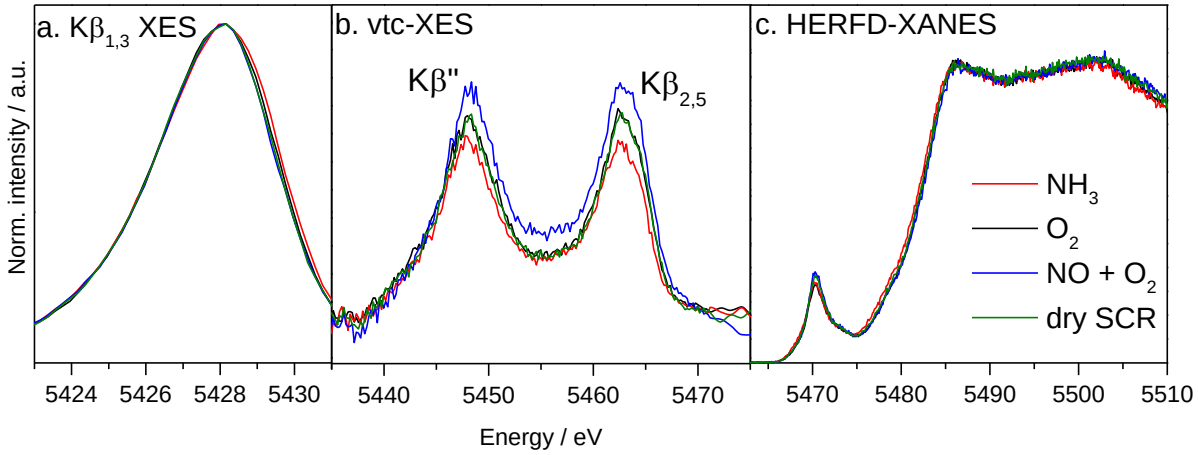

Figure 9. *Operando* (a) Kβ$_{1,3}$ XES, (b) vtc-XES and (c) HERFD-XANES spectra of the grafted VT-gr catalyst during dry SCR (1000 ppm NO, 1000 ppm NH_3, 5% O_2 in He, no water vapor) and in related model gas mixtures (diluted with He). Temperature 400 °C.

In spite of high SCR activity of both grafted catalysts (Fig. 2) and high V dispersion, the spectral response to different SCR-related gas feeds is significantly weaker than in the case of the impregnated catalyst. Reduction of V sites could be clearly identified only in NH_3/He feed, and the changes in the XANES spectra were marginal with virtually no change in the V coordination environment. Weak changes also resulted in high error bars during determination of oxidation state via the variograms. In this case, Kβ$_{1,3}$ XES appears to be an easier way to

quantify the oxidation state of V. Regarding the coordination of V sites in the grafted catalysts, V sites demonstrate different coordination geometries. CN 5 is reported for VWT-gr and CN 6 for VT-gr catalysts, which agrees with the differences observed in the Raman spectra. No significant changes in the coordination geometry were observed, substantiating the role of V active species especially as redox sites and less evident as direct NH_x/NO_x adsorption sites.

4. Conclusions

High energy resolution fluorescence detection allowed us to probe the oxidation state of V under realistic conditions and in the presence of W and Ti which are required in active and stable NH_3-SCR catalysts. The obtained results reveal redox dynamics of V sites typical also for metal sites in Fe- and Cu-zeolite catalysts during NH_3-SCR.[34,35,65] Most importantly, partial reduction of V species in the NH_3-SCR feed was found. On the other hand, contrary to the SCR over zeolites, hardly any changes in the first coordination shell of V sites could be found using vtc-XES spectra alone in line with a weak spectral response of species outside the first coordination shell of V (e.g. Brønsted-bound ammonia). Hence, the X-ray spectra of V sites measured under SCR and related conditions cannot not be used alone to prove ammonia adsorption on Brønsted or Lewis vanadium sites and need to be complemented by techniques looking at NH_3, e.g. DRIFTS and nitrogen K edge (soft X-ray) XAS/XES.[69]

$K\beta_{1,3}$ XES proved to be the most sensitive and straightforward tool to quantify oxidation state of V species, mostly because it less dependent on the nature/geometry of V species which hinders XANES analysis. In future, more substantial calculations both of XANES and vtc-XES data as well as combination with NH_3-sensitive techniques such as DRIFTS may allow drawing further conclusions. Taking into account the fact that $K\beta_{1,3}$ XES is recorded as a part of the HERFD-XANES measurement protocol it is the also the fastest way to obtain oxidation state of V in VWT catalysts. Additional advantage of using V $K\beta_{1,3}$ XES spectra is that they

can be obtained within several minutes using state-of-the-art laboratory XAS/XES spectrometers.[70] Compared to widely used EPR and Raman spectroscopy, XAS and XES may offer more precise and straightforward quantification of V oxidation state since species with all relevant oxidation states (V^{5+}, V^{4+}, V^{3+}) can be detected. Moreover, V XES can be easily combined with Ti XES measurements, which may potentially provide further information on the role of titania (such as interaction with V and / or providing NH_3 adsorption sites) in VWT catalysts.

Supporting Information

The following additional information is given in the SI: evaluation of potential beam damage, X-ray diffractograms and Raman spectra of the studied catalysts; V active site models; variograms extracted from *operando* HERFD-XANES of VWT-gr and VT-gr catalysts, input files for vtc-XES calculations.

Acknowledgments

The experiments were performed on beamline ID26 at the European Synchrotron Radiation Facility (ESRF), Grenoble, France. We are grateful to Dr. P. Glatzel, Dr. R. Baran and T. Bodhan at the ESRF for providing assistance in using beamline ID26. This study is the extension of a research work supported by the Forschungsvereinigung Verbrennungskraftmaschinen e. V. (FVV, Frankfurt). We thank A. Feiling and C. Beidl (both TU Darmstadt) as well as the FVV work group led by U. Gärtner (Daimler AG) for discussion and support. The authors thank E. Japke for VWT and VWT-gr synthesis, VWT catalytic test and help during the synchrotron measurements, Dr. J. Strunk (MPI-CEC) for providing the VT-gr sample and Ying-Zhao Ma (KIT) for assistance during the VWT-gr sample preparation. Dr. G. Giuli (Unicam) is kindly acknowledged for providing the V-bearing model compounds. P. Sprenger and M. Stehle (KIT) are acknowledged for assistance during Raman measurements. Authors thank the German Research Foundation (DFG) for granting the funds

for the Raman spectrometer (INST 121384/73-1) and the thermal analysis instrument (INST 121384/70-1). L.Z. is grateful to China Scholarship Council (CSC) for a PhD scholarship. The authors acknowledge support by the state of Baden-Württemberg through bwHPC (bwunicluster and JUSTUS, RV bw17D011).

References

(1) Deutschmann, O.; Grunwaldt, J.-D. Abgasnachbehandlung in Mobilen Systemen: Stand der Technik, Herausforderungen und Perspektiven (Exhaust Gas Aftertreatment in Mobile Systems: Status, Challenges, and Perspectives, in German). *Chem. Ing. Tech.* **2013**, *85* (5), 595–617. https://doi.org/10.1002/cite.201200188.

(2) Gao, F.; Kwak, J. H.; Szanyi, J.; Peden, C. H. F. Current Understanding of Cu-Exchanged Chabazite Molecular Sieves for Use as Commercial Diesel Engine DeNO(x) Catalysts. *Top. Catal.* **2013**, *56* (15–17), 1441–1459. https://doi.org/10.1007/s11244-013-0145-8.

(3) Ruggeri, M. P.; Nova, I.; Tronconi, E. Experimental Study of the NO Oxidation to NO_2 Over Metal Promoted Zeolites Aimed at the Identification of the Standard SCR Rate Determining Step. *Top. Catal.* **2013**, *56* (1–8), 109–113. https://doi.org/10.1007/s11244-013-9937-0.

(4) Marberger, A.; Elsener, M.; Ferri, D.; Kröcher, O. VOx Surface Coverage Optimization of V_2O_5/WO_3-TiO_2 SCR Catalysts by Variation of the V Loading and by Aging. *Catalysts* **2015**, *5* (4), 1704–1720. https://doi.org/10.3390/catal5041704.

(5) He, Y.; Ford, M. E.; Zhu, M.; Liu, Q.; Tumuluri, U.; Wu, Z.; Wachs, I. E. Influence of Catalyst Synthesis Method on Selective Catalytic Reduction (SCR) of NO by NH_3 with V_2O_5-WO_3/TiO_2 Catalysts. *Appl. Catal. B Environ.* **2016**, *193*, 141–150. https://doi.org/10.1016/j.apcatb.2016.04.022.

(6) Rammelt, T.; Torkashvand, B.; Hauck, C.; Böhm, J.; Gläser, R.; Deutschmann, O. Nitric Oxide Reduction of Heavy-Duty Diesel Off-Gas by NH_3-SCR in Front of the Turbocharger. *Emiss. Control Sci. Technol.* **2017**, *3* (4), 275–288. https://doi.org/10.1007/s40825-017-0078-y.

(7) Japke, E.; Casapu, M.; Trouillet, V.; Deutschmann, O.; Grunwaldt, J.-D. Soot and Hydrocarbon Oxidation over Vanadia-Based SCR Catalysts. *Catal. Today* **2015**, *258*, 461–469. https://doi.org/10.1016/j.cattod.2015.04.020.

(8) Forzatti, P. Present Status and Perspectives in De-NOx SCR Catalysis. *Appl. Catal. A* **2001**, *222* (1–2), 221–236. https://doi.org/10.1016/S0926-860X(01)00832-8.

(9) Lietti, L.; Forzatti, P.; Bregani, F. Steady-State and Transient Reactivity Study of TiO_2-Supported V_2O_5−WO_3 De-NOx Catalysts: Relevance of the Vanadium−Tungsten Interaction on the Catalytic Activity. *Ind. Eng. Chem. Res.* **1996**, *35* (11), 3884–3892. https://doi.org/10.1021/ie960158l.

(10) Kompio, P. G. W. A.; Brückner, A.; Hipler, F.; Auer, G.; Löffler, E.; Grünert, W. A New View on the Relations between Tungsten and Vanadium in $V_2O_5WO_3$/TiO_2 Catalysts for the Selective Reduction of NO with NH_3. *J. Catal.* **2012**, *286*, 237–247. https://doi.org/10.1016/j.jcat.2011.11.008.

(11) Amiridis, M. D.; Duevel, R. V.; Wachs, I. E. The Effect of Metal Oxide Additives on the Activity of V_2O_5/TiO_2 Catalysts for the Selective Catalytic Reduction of Nitric Oxide by Ammonia. *Appl. Catal. B* **1999**, *20* (2), 111–122. https://doi.org/10.1016/S0926-3373(98)00101-5.

(12) Murkute, A. D.; Vanderwiel, D. Active Sites Evaluation of Vanadia Based Powdered and Extruded SCR Catalysts Prepared on Commercial Titania. *Catal. Lett.* **2015**, *145* (6), 1224–1236. https://doi.org/10.1007/s10562-015-1511-x.

(13) Baiker, A.; Handy, B.; Nickl, J.; Schraml-Marth, M.; Wokaun, A. Selective Catalytic Reduction of Nitric Oxide over Vanadia Grafted on Titania. Influence of Vanadia Loading on

Structural and Catalytic Properties of Catalysts. *Catal. Lett.* **1992**, *14* (1), 89–99. https://doi.org/10.1007/BF00764222.

(14) Topsøe, N.-Y. Mechanism of the Selective Catalytic Reduction of Nitric Oxide by Ammonia Elucidated by in Situ On-Line Fourier Transform Infrared Spectroscopy. *Science* **1994**, *265* (5176), 1217–1219. https://doi.org/10.1126/science.265.5176.1217.

(15) Topsøe, N. Y.; Dumesic, J. A.; Topsøe, H. Vanadia-Titania Catalysts for Selective Catalytic Reduction of Nitric-Oxide by Ammonia. *J. Catal.* **1995**, *151* (1), 241–252. https://doi.org/10.1006/jcat.1995.1025.

(16) Anstrom, M.; Topsøe, N.-Y.; Dumesic, J. A. Density Functional Theory Studies of Mechanistic Aspects of the SCR Reaction on Vanadium Oxide Catalysts. *J. Catal.* **2003**, *213* (2), 115–125. https://doi.org/10.1016/S0021-9517(02)00031-3.

(17) Yin, X.; Han, H.; Miyamoto, A. Active Site and Mechanism of the Selective Catalytic Reduction of NO by NH_3 over V_2O_5: A Periodic First-Principles Study. *Phys. Chem. Chem. Phys.* **2000**, *2* (18), 4243–4248. https://doi.org/10.1039/b003838p.

(18) Ramis, G.; Yi, L.; Busca, G. Ammonia Activation over Catalysts for the Selective Catalytic Reduction of NOx and the Selective Catalytic Oxidation of NH_3. An FT-IR Study. *Catal. Today* **1996**, *28* (4), 373–380. https://doi.org/10.1016/S0920-5861(96)00050-8.

(19) Marberger, A.; Ferri, D.; Elsener, M.; Kröcher, O. The Significance of Lewis Acid Sites for the Selective Catalytic Reduction of Nitric Oxide on Vanadium-Based Catalysts. *Angew. Chem. Int. Ed.* **2016**. https://doi.org/10.1002/anie.201605397.

(20) Vittadini, A.; Casarin, M.; Selloni, A. First Principles Studies of Vanadia−Titania Monolayer Catalysts: Mechanisms of NO Selective Reduction. *J. Phys. Chem. B* **2005**, *109* (5), 1652–1655. https://doi.org/10.1021/jp044752h.

(21) Tronconi, E.; Nova, I.; Ciardelli, C.; Chatterjee, D.; Weibel, M. Redox Features in the Catalytic Mechanism of the "Standard" and "Fast" NH_3-SCR of NOx over a V-Based Catalyst Investigated by Dynamic Methods. *J. Catal.* **2007**, *245* (1), 1–10. https://doi.org/10.1016/j.jcat.2006.09.012.

(22) Due-Hansen, J.; Rasmussen, S. B.; Mikolajska, E.; Bañares, M. A.; Ávila, P.; Fehrmann, R. Redox Behaviour of Vanadium during Hydrogen–Oxygen Exposure of the V_2O_5-WO_3/TiO_2 SCR Catalyst at 250°C. *Appl. Catal. B* **2011**, *107* (3–4), 340–346. https://doi.org/10.1016/j.apcatb.2011.07.034.

(23) Vuong, T. H.; Radnik, J.; Rabeah, J.; Bentrup, U.; Schneider, M.; Atia, H.; Armbruster, U.; Grünert, W.; Brückner, A. Efficient $VO_x/Ce_{1-x}Ti_xO_2$ Catalysts for Low-Temperature NH_3-SCR: Reaction Mechanism and Active Sites Assessed by in Situ/Operando Spectroscopy. *ACS Catal.* **2017**, *7* (3), 1693–1705. https://doi.org/10.1021/acscatal.6b03223.

(24) Arnarson, L.; Falsig, H.; Rasmussen, S. B.; Lauritsen, J. V.; Moses, P. G. The Reaction Mechanism for the SCR Process on Monomer V^{5+} Sites and the Effect of Modified Brønsted Acidity. *Phys Chem Chem Phys* **2016**, *18* (25), 17071–17080. https://doi.org/10.1039/C6CP02274J.

(25) Rasmussen, S. B.; Portela, R.; Bazin, P.; Ávila, P.; Bañares, M. A.; Daturi, M. Transient Operando Study on the NH_3/NH_4^+ Interplay in V-SCR Monolithic Catalysts. *Appl. Catal. B Environ.* **2018**, *224*, 109–115. https://doi.org/10.1016/j.apcatb.2017.10.026.

(26) Doronkin, D. E.; Casapu, M.; Günter, T.; Müller, O.; Frahm, R.; Grunwaldt, J.-D. Operando Spatially- and Time-Resolved XAS Study on Zeolite Catalysts for Selective Catalytic Reduction of NO_x by NH_3. *J. Phys. Chem. C* **2014**, *118* (19), 10204–10212. https://doi.org/10.1021/jp5028433.

(27) Günter, T.; Doronkin, D. E.; Boubnov, A.; Carvalho, H. W. P.; Casapu, M.; Grunwaldt, J.-D. The SCR of NOx with NH_3 Examined by Novel X-Ray Emission and X-Ray Absorption Methods. *Top. Catal.* **2016**, *59* (10–12), 866–874. https://doi.org/10.1007/s11244-016-0561-7.

(28) Wong, J.; Lytle, F. W.; Messmer, R. P.; Maylotte, D. H. K -Edge Absorption Spectra of Selected Vanadium Compounds. *Phys. Rev. B* **1984**, *30* (10), 5596–5610. https://doi.org/10.1103/PhysRevB.30.5596.

(29) Safonova, O. V.; Florea, M.; Bilde, J.; Delichere, P.; Millet, J. M. M. Local Environment of Vanadium in V/Al/O-Mixed Oxide Catalyst for Propane Ammoxidation: Characterization by in Situ Valence-to-Core X-Ray Emission Spectroscopy and X-Ray Absorption Spectroscopy. *J. Catal.* **2009**, *268* (1), 156–164. https://doi.org/http://dx.doi.org/10.1016/j.jcat.2009.09.014.

(30) Yamamoto, T.; Nanbu, F.; Tanaka, T.; Kawai, J. Quantitative Chemical State Analysis of Supported Vanadium Oxide Catalysts by High Resolution Vanadium Kα Spectroscopy. *Anal. Chem.* **2011**, *83* (5), 1681–1687. https://doi.org/10.1021/ac102681z.

(31) Burkardt, A.; Weisweiler, W.; van den Tillaart, J. A. A.; Schäfer-Sindlinger, A.; Lox, E. S. Influence of the V2O5 Loading on the Structure and Activity of V_2O_5/TiO_2 SCR Catalysts for Vehicle Application. *Top. Catal.* **2001**, *16* (1), 369–375. https://doi.org/10.1023/A:1016673418398.

(32) Beale, A. M.; Lezcano-Gonzalez, I.; Maunula, T.; Palgrave, R. G. Development and Characterization of Thermally Stable Supported V–W–TiO_2 Catalysts for Mobile NH_3 –SCR Applications. *Catal. Struct. React.* **2015**, *1* (1), 25–34. https://doi.org/10.1179/2055075814Y.0000000005.

(33) Glatzel, P.; Bergmann, U. High Resolution 1s Core Hole X-Ray Spectroscopy in 3d Transition Metal Complexes—Electronic and Structural Information. *Coord. Chem. Rev.* **2005**, *249* (1–2), 65–95. https://doi.org/10.1016/j.ccr.2004.04.011.

(34) Boubnov, A.; Carvalho, H. W. P.; Doronkin, D. E.; Günter, T.; Gallo, E.; Atkins, A. J.; Jacob, C. R.; Grunwaldt, J.-D. Selective Catalytic Reduction of NO Over Fe-ZSM-5: Mechanistic Insights by Operando HERFD-XANES and Valence-to-Core X-Ray Emission Spectroscopy. *J. Am. Chem. Soc.* **2014**, *136* (37), 13006–13015. https://doi.org/10.1021/ja5062505.

(35) Günter, T.; Carvalho, H. W. P.; Doronkin, D. E.; Sheppard, T.; Glatzel, P.; Atkins, A. J.; Rudolph, J.; Jacob, C. R.; Casapu, M.; Grunwaldt, J.-D. Structural Snapshots of the SCR Reaction Mechanism on Cu-SSZ-13. *Chem Commun* **2015**, *51* (44), 9227–9230. https://doi.org/10.1039/C5CC01758K.

(36) Giordanino, F.; Borfecchia, E.; Lomachenko, K. A.; Lazzarini, A.; Agostini, G.; Gallo, E.; Soldatov, A. V.; Beato, P.; Bordiga, S.; Lamberti, C. Interaction of NH_3 with Cu-SSZ-13 Catalyst: A Complementary FTIR, XANES, and XES Study. *J. Phys. Chem. Lett.* **2014**, *5* (9), 1552–1559. https://doi.org/10.1021/jz500241m.

(37) Reiche, M.; Ortelli, E.; Baiker, A. Vanadia Grafted on TiO_2–SiO_2, TiO_2 and SiO_2 Aerogels Structural Properties and Catalytic Behaviour in Selective Reduction of NO by NH_3. *Appl. Catal. B Environ.* **1999**, *23* (2–3), 187–203. https://doi.org/10.1016/S0926-3373(99)00076-4.

(38) Brunauer, S.; Emmett, P. H.; Teller, E. Adsorption of Gases in Multimolecular Layers. *J. Am. Chem. Soc.* **1938**, *60* (2), 309–319. https://doi.org/10.1021/ja01269a023.

(39) Feiling, A.; Japke, E.; Beidl, C.; Deutschmann, O.; Grunwaldt, J.-D. PM Reduktion Über V-SCR; *FVV Report* **2016,** 1146.

(40) Farges, F.; Brown, G. E.; Rehr, J. J. Coordination Chemistry of Ti(IV) in Silicate Glasses and Melts: I. XAFS Study of Titanium Coordination in Oxide Model Compounds. *Geochim. Cosmochim. Acta* **1996**, *60* (16), 3023–3038. https://doi.org/10.1016/0016-7037(96)00144-5.

(41) Giuli, G.; Paris, E.; Mungall, J.; Romano, C.; Dingwell, D. V Oxidation State and Coordination Number in Silicate Glasses by XAS. *Am. Mineral.* **2004**, *89* (11–12), 1640–1646. https://doi.org/10.2138/am-2004-11-1208.

(42) Wojdyr, M. Fityk: A General-Purpose Peak Fitting Program. *J. Appl. Crystallogr.* **2010**, *43* (5), 1126–1128. https://doi.org/10.1107/S0021889810030499.

(43) Gallo, E.; Glatzel, P. Valence to Core X-Ray Emission Spectroscopy. *Adv. Mater.* **2014**, *26* (46), 7730–7746. https://doi.org/10.1002/adma.201304994.

(44) Grunwaldt, J.-D.; Caravati, M.; Hannemann, S.; Baiker, A. X-Ray Absorption Spectroscopy under Reaction Conditions: Suitability of Different Reaction Cells for Combined Catalyst Characterization and Time-Resolved Studies. *Phys Chem Chem Phys* **2004**, *6* (11), 3037–3047. https://doi.org/10.1039/B403071K.

(45) Benzi, F.; Giuli, G.; Della Longa, S.; Paris, E. Vanadium K-Edge XANES in Vanadium-Bearing Model Compounds: A Full Multiple Scattering Study. *J. Synchrotron Radiat.* **2016**, *23* (4), 947–952. https://doi.org/10.1107/S1600577516008134.

(46) Newville, M. IFEFFIT : Interactive XAFS Analysis and FEFF Fitting. *J. Synchrotron Radiat.* **2001**, *8* (2), 322–324. https://doi.org/10.1107/S0909049500016964.

(47) Kresse, G.; Furthmüller, J. Efficient Iterative Schemes for Ab Initio Total-Energy Calculations Using a Plane-Wave Basis Set. *Phys. Rev. B* **1996**, *54* (16), 11169–11186. https://doi.org/10.1103/PhysRevB.54.11169.

(48) Wellendorff, J.; Lundgaard, K. T.; Møgelhøj, A.; Petzold, V.; Landis, D. D.; Nørskov, J. K.; Bligaard, T.; Jacobsen, K. W. Density Functionals for Surface Science: Exchange-Correlation Model Development with Bayesian Error Estimation. *Phys. Rev. B* **2012**, *85* (23). https://doi.org/10.1103/PhysRevB.85.235149.

(49) Arnarson, L.; Rasmussen, S. B.; Falsig, H.; Lauritsen, J. V.; Moses, P. G. Coexistence of Square Pyramidal Structures of Oxo Vanadium (+5) and (+4) Species Over Low-Coverage VO_x/TiO_2 (101) and (001) Anatase Catalysts. *J. Phys. Chem. C* **2015**, *119* (41), 23445–23452. https://doi.org/10.1021/acs.jpcc.5b06132.

(50) Yin, X.; Han, H.; Gunji, I.; Endou, A.; Cheettu Ammal, S. S.; Kubo, M.; Miyamoto, A. NH_3 Adsorption on the Brönsted and Lewis Acid Sites of V_2O_5 (010): A Periodic Density Functional Study. *J. Phys. Chem. B* **1999**, *103* (22), 4701–4706. https://doi.org/10.1021/jp990363p.

(51) Rehr, J. J.; Kas, J. J.; Vila, F. D.; Prange, M. P.; Jorissen, K. Parameter-Free Calculations of X-Ray Spectra with FEFF9. *Phys. Chem. Chem. Phys.* **2010**, *12* (21), 5503–5513. https://doi.org/10.1039/B926434E.

(52) Ohno, T.; Sarukawa, K.; Tokieda, K.; Matsumura, M. Morphology of a TiO_2 Photocatalyst (Degussa, P-25) Consisting of Anatase and Rutile Crystalline Phases. *J. Catal.* **2001**, *203* (1), 82–86. https://doi.org/10.1006/jcat.2001.3316.

(53) Balachandran, U.; Eror, N. G. Raman Spectra of Titanium Dioxide. *J. Solid State Chem.* **1982**, *42* (3), 276–282. https://doi.org/10.1016/0022-4596(82)90006-8.

(54) Frank, O.; Zukalova, M.; Laskova, B.; Kürti, J.; Koltai, J.; Kavan, L. Raman Spectra of Titanium Dioxide (Anatase, Rutile) with Identified Oxygen Isotopes (16, 17, 18). *Phys. Chem. Chem. Phys.* **2012**, *14* (42), 14567. https://doi.org/10.1039/c2cp42763j.

(55) Rasmussen, S. B.; Mikolajska, E.; Daturi, M.; Bañares, M. A. Structural Characteristics of an Amorphous VPO Monolayer on Alumina for Propane Ammoxidation. *Catal. Today* **2012**, *192* (1), 96–103. https://doi.org/10.1016/j.cattod.2012.03.065.

(56) Went, G. T.; Oyama, S. T.; Bell, A. T. Laser Raman Spectroscopy of Supported Vanadium Oxide Catalysts. *J. Phys. Chem.* **1990**, *94* (10), 4240–4246. https://doi.org/10.1021/j100373a067.

(57) Piumetti, M.; Bensaid, S.; Fino, D.; Russo, N. Catalysis in Diesel Engine NO_x Aftertreatment: A Review. *Catal. Struct. React.* **2015**, *1* (4), 155–173. https://doi.org/10.1080/2055074X.2015.1105615.

(58) Wierzbicki, D.; Baran, R.; Dębek, R.; Motak, M.; Gálvez, M. E.; Grzybek, T.; Da Costa, P.; Glatzel, P. Examination of the Influence of La Promotion on Ni State in Hydrotalcite-Derived Catalysts under CO_2 Methanation Reaction Conditions: Operando X-Ray Absorption and Emission Spectroscopy Investigation. *Appl. Catal. B* **2018**, *232*, 409–419. https://doi.org/10.1016/j.apcatb.2018.03.089.

(59) Wilke, M.; Farges, F.; Petit, P.-E.; Brown Jr., G. E.; Martin, F. Oxidation State and Coordination of Fe in Minerals: An Fe K-XANES Spectroscopic Study. *Am. Mineral.* **2001**, *86*, 714–730. https://doi.org/10.2138/am-2001-5-612.

(60) Westre, T. E.; Kennepohl, P.; DeWitt, J. G.; Hedman, B.; Hodgson, K. O.; Solomon, E. I. A Multiplet Analysis of Fe K-Edge 1s → 3d Pre-Edge Features of Iron Complexes. *J. Am. Chem. Soc.* **1997**, *119* (27), 6297–6314. https://doi.org/10.1021/ja964352a.

(61) Vankó, G.; Neisius, T.; Molnár, G.; Renz, F.; Kárpáti, S.; Shukla, A.; de Groot, F. M. F. Probing the 3d Spin Momentum with X-Ray Emission Spectroscopy: The Case of Molecular-Spin Transitions. *J. Phys. Chem. B* **2006**, *110* (24), 11647–11653. https://doi.org/10.1021/jp0615961.

(62) Vuong, T. H.; Radnik, J.; Kondratenko, E.; Schneider, M.; Armbruster, U.; Brückner, A. Structure-Reactivity Relationships in $VO_x/Ce_xZr_{1-x}O_2$ Catalysts Used for Low-Temperature NH_3-SCR of NO. *Appl. Catal. B* **2016**, *197*, 159–167. https://doi.org/10.1016/j.apcatb.2016.03.063.

(63) Schindler, M.; Hawthorne, F. C.; Baur, W. H. Crystal Chemical Aspects of Vanadium: Polyhedral Geometries, Characteristic Bond Valences, and Polymerization of (VO_n) Polyhedra. *Chem. Mater.* **2000**, *12* (5), 1248–1259. https://doi.org/10.1021/cm990490y.

(64) Janssens, T. V. W.; Falsig, H.; Lundegaard, L. F.; Vennestrøm, P. N. R.; Rasmussen, S. B.; Moses, P. G.; Giordanino, F.; Borfecchia, E.; Lomachenko, K. A.; Lamberti, C.; et al. A

Consistent Reaction Scheme for the Selective Catalytic Reduction of Nitrogen Oxides with Ammonia. *ACS Catal.* **2015**, *5* (5), 2832–2845. https://doi.org/10.1021/cs501673g.

(65) Paolucci, C.; Verma, A. A.; Bates, S. A.; Kispersky, V. F.; Miller, J. T.; Gounder, R.; Delgass, W. N.; Ribeiro, F. H.; Schneider, W. F. Isolation of the Copper Redox Steps in the Standard Selective Catalytic Reduction on Cu-SSZ-13. *Angew. Chem. Int. Ed.* **2014**, *53* (44), 11828–11833. https://doi.org/10.1002/anie.201407030.

(66) Zhu, M.; Lai, J.-K.; Tumuluri, U.; Wu, Z.; Wachs, I. E. Nature of Active Sites and Surface Intermediates during SCR of NO with NH_3 by Supported V_2O_5–WO_3/TiO_2 Catalysts. *J. Am. Chem. Soc.* **2017**, *139* (44), 15624–15627. https://doi.org/10.1021/jacs.7b09646.

(67) Morterra, C.; Ghiotti, G.; Garrone, E.; Fisicaro, E. Spectroscopic Study of Anatase Properties. Part 3.—Surface Acidity. *J. Chem. Soc. Faraday Trans. 1 Phys. Chem. Condens. Phases* **1980**, *76* (0), 2102-. https://doi.org/10.1039/f19807602102.

(68) Odenbrand, C. U. I.; Brandin, J. G. M.; Busca, G. Surface Acidity of Silica-Titania Mixed Oxides. *J. Catal.* **1992**, *135* (2), 505–517. https://doi.org/10.1016/0021-9517(92)90050-R.

(69) Weinhardt, L.; Ertan, E.; Iannuzzi, M.; Weigand, M.; Fuchs, O.; Bär, M.; Blum, M.; Denlinger, J. D.; Yang, W.; Umbach, E.; et al. Probing Hydrogen Bonding Orbitals: Resonant Inelastic Soft X-Ray Scattering of Aqueous NH_3. *Phys. Chem. Chem. Phys.* **2015**, *17* (40), 27145–27153. https://doi.org/10.1039/C5CP04898B.

(70) Jahrman, E. P.; Holden, W. M.; Ditter, A. S.; Mortensen, D. R.; Seidler, G. T.; Fister, T. T.; Kozimor, S. A.; Piper, L. F. J.; Rana, J.; Hyatt, N. C.; et al. An Improved Laboratory-Based x-Ray Absorption Fine Structure and x-Ray Emission Spectrometer for Analytical Applications in Materials Chemistry Research. *Rev. Sci. Instrum.* **2019**, *90* (2), 024106. https://doi.org/10.1063/1.5049383.

TOC Graphic